Available online at www.sciencedirect.com
ScienceDirect
Journal of the European Ceramic Society 31 (2011) 3119–3125
www.elsevier.com/locate/jeurceramsoc

Assessment of structurally stable cubic $Bi_{12}TiO_{20}$ as intermediate temperature solid oxide fuels electrolyte

Yu-Lin Kuo [a,*], Li-Der Liu [b], Sung-En Lin [b], Chia-Hao Chou [a], Weng-Cheng J. Wei [b]

[a] *Department of Mechanical Engineering, National Taiwan University of Science and Technology, Taipei 106, Taiwan*
[b] *Department of Materials Science and Engineering, National Taiwan University, Taipei 106, Taiwan*

Available online 20 May 2011

Abstract

Colloid processing and subsequent pressure filtration were used to prepare 14.3 mol% TiO_2 doped Bi_2O_3 ($Bi_{12}TiO_{20}$, 14BTO) as solid oxide fuel cell electrolyte. Materials characterization and electrical behaviors of 14BTO samples were investigated by X-ray diffraction (XRD), scanning electron microscopy (SEM) and two-point probe DC conductivity. A pure 14BTO with a cubic sillenite single phase was prepared at the sintering process of 850 °C with a high relative sintered density of 96.82%. In situ and batch-type long-term conductivity measurements at 600 °C were carried out to verify the possible reason of degradation. Additional reduction–oxidation tests under CH_4 atmosphere by thermogravimetric analysis (TGA) revealed possible application temperature of 14BTO electrolytes below 700 °C.

Keywords: TiO_2; Bi_2O_3; Pressure filtration; Solid oxide fuel cells (SOFCs); Electrolytes

1. Introduction

δ-Cubic Bi_2O_3 is well known for its exceptional ionic conductivity of oxygen ions. The material has been extensively explored through analytic computer simulations and experimental analysis to access its applicability for SOFC electrolyte applications. The problems of using Bi_2O_3 as SOFC electrolyte currently consists of low chemical stability in reduction atmospheres and narrow phase stability temperature range. It has been reported that Bi_2O_3 becomes unstable when the oxygen partial pressure is below 10^{-6} Pa at 700 °C.[1] As a result, an additional barrier layer is required to prevent Bi_2O_3-based electrolyte surface from being reduced. Through suitable doping, the high ionic conduction phase can be stabilized to broaden the working range to lower temperatures.[1–4]

The trivalent M^{3+} lanthanides were largely exploited their phase stability and conductivity on the doped structures.[5–7] In the work by Wachsman et al.,[8,2] substitution of lanthanides oxides with various ionic radii reduced the polarizability of the ionic structure were reported elsewhere. Experiments have also shown that the trivalent doped structures were prone to a conductivity decay over long-term aging.[2] Some referred the decay is due to the ordering of dopant cations,[9,10] while others proposed the ordering of oxygen vacancies revealing forms of superlattice structure from electron diffraction patterns,[11,12] both act to reduce the high disorder of anion lattice structure that accommodate for high O^{2-} mobility. Nevertheless, the lanthanide dopants are capable of stabilizing the cubic δ-structure while maintaining conductivity as high as 0.23 S/cm at 600 °C for 20 mol% Er_2O_3-doped Bi_2O_3 system.[13]

The tetravalent and pentavalent doped Bi_2O_3 were each surveyed few decades ago by Esaka and Iwahara et al.[14,15] Unlike the trivalent dopants, the aliovalent dopants would result in defect balance equations that fill up the pre-existing oxygen vacancies, hence stabilizing the high temperature bismuth oxide structure. A dominant defect balance for doping tetravalent MO_2 oxides into δ-Bi_2O_3 structure would appear as:

$$2MO_2 + V_O^{\bullet\bullet} \rightarrow 2M_{Bi}^{\bullet} + 4O_O^X \quad (1)$$

Due to stoichiometry of the tetravalent oxides, it would fill up one oxygen vacancy per two M^{4+} cation dopants. Of the four different tetravalent cations (Te, Ti, Sn, Zr) reported,[14] Ti^{4+} presented a relatively small ionic radius at 0.60 Å. At 600 °C, Bi_2O_3 doped with 57–75 mol% TiO_2 exhibited conductivities in the order of 10^{-5} S/cm.[14] The conductivity values were far from satisfactory. In TiO_2–Bi_2O_3 binary phase diagram, a cubic structured $Bi_{12}TiO_{20}$ with 14.3 mol% TiO_2 (14BTO) is

* Corresponding author. Tel.: +886 2 27376784; fax: +886 2 27376460.
E-mail address: ylkuo@mail.ntust.edu.tw (Y.-L. Kuo).

0955-2219/$ – see front matter © 2011 Elsevier Ltd. All rights reserved.
doi:10.1016/j.jeurceramsoc.2011.04.039

present and stable from room temperature up to its melting point (~875 °C).[16] $Bi_{12}TiO_{20}$ is a common photocatalyst material of body-centered cubic (bcc) structure with a combination of interesting optoelectronic properties.[17–21] However, little is known on the conductive properties and stability properties as SOFC electrolyte.

In this study, the material investigated is strictly focused on preparation and characterization of 14BTO. According to our previous work, colloid processing followed with pressure filtration[22,23] was executed to obtain the samples with a higher quality. XRD and SEM were used to examine the microstructural morphology, crystal structure, and surface porosity of the sintered pellets. Archimedes method was applied to measure the relative densities of the samples. In situ and batch-type long-term conductivity measurements as long as 1344 h at 600 °C were carried out to verify the possible reason of degradation. Additional reduction–oxidation tests under CH_4 atmosphere by TGA were accomplished to estimate possible application temperature of the samples.

2. Experimental

Bi_2O_3 powder (99.9%, Solartech, Taiwan) and TiO_2 powder (99.9%, Alfa Aesar, USA) were used to prepare TiO_2-doped Bi_2O_3 samples by colloidal process-pressure filtration. As purchased TiO_2 and Bi_2O_3 powder were separately dispersed in de-ionized water with 1 wt% (based on oxide powder) of D-134 dispersant (ammonium salt homopolymer with a 2-propenoic acid group, Dai-Ichi Kogyo Seiyaku Co. Ltd., Japan) and then ball-milled for 24 h to ensure well-mixed slurries. The powders were verified by XRD to be α-monoclinic Bi_2O_3 and tetragonal anatase TiO_2. By SEM, the diameters of the starting powder were 2–3 μm for Bi_2O_3 and sub-micron for TiO_2. After 1 day of ball-milling, narrower distributions were obtained at 2.2 μm and 0.5 μm for Bi_2O_3 and TiO_2, respectively. Stoichiometric 14.3 mol% of titania slurry was then added into the Bi_2O_3 slurry for another 2 h of ball-mill mixing and then pressure filtrated in a self-designed acrylic mold at 10 atm followed by 2 h sintering of the green disks at 775 °C, 800 °C, 825 °C, and 850 °C with a heating rate of 10 °C min^{-1}. 14BTO powder was also prepared for the die-pressing at 140 MPa as the comparison.

2.1. Microstructural analysis and conductivity measurement

The exact crystal phases of the material were obtained by RIGAKU RTP 300 XRD. The incident beam was Cu Kα characteristic X-ray at 40 kV and 100 mA. Secondary electron images from SEM were used to observe the microstructural morphology and grain size of the sample. The sintered densities of the 14BTO disks were then derived by the Archimedes relations.

Conductivities of the samples were measured at temperatures ranging from 500 °C to 700 °C. Platinum electrodes of 0.1 cm diameter were secured via Heraeus CL11-5100 Pt adhesive paste on either sides of the sample pellet and held at raised temperature for 1 h. Two-point probe DC conductivity was measured accordingly. Long-term conductivity measurements at 600 °C by in situ and batch-type methods are carried out to verify the possible reason of degradation of 14BTO samples. In situ long-term conductivity measurement was continuously recorded in 24 h. Aging test of 14BTO samples placed at the furnace with an aging temperature of 600 °C was performed for the batch-type long-term conductivity, and each sample was taken out from the furnace in the specific time for the further conductivity measurement.

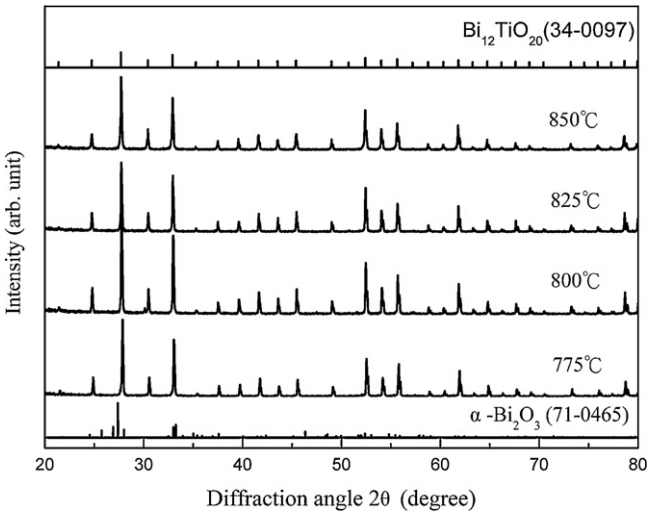

Fig. 1. XRD spectra of 14BTO samples sintered at various temperatures for 2 h.

The behaviors of reduction–oxidation of 14BTO samples at temperatures of 700–800 °C under CH_4 atmosphere was carried out by TGA. The ramping process was firstly heating to the fixed temperature under N_2 atmosphere. Then, 20% CH_4 inlet gas with a flow rate of 20 sccm was introduced to TGA chamber for the reduction stability test. After at least 1 h reduction, air gas was subsequently introduced to oxide the samples. In order to prevent the combustion reaction between CH_4 and O_2 gases during the operation, N_2 purge gas was necessarily introduced for 10 min prior to the inlet of air gas.

3. Results and discussion

3.1. Structural identification

Sintered samples at temperatures of 775 °C, 800 °C, 825 °C, and 850 °C were examined by XRD from the pressure filtration process as shown in Fig. 1. All the cases revealed a single phase $Bi_{12}TiO_{20}$ with a cubic sillenite structure (JCPDS # 34-0097) and the strongest diffraction peak of (3 1 0) plane is recorded at the 2θ of 27.7°. Additionally, 14BTO treated at 850 °C for 2 h shows the smallest mismatch on peak location with single crystal 14BTO produced by Czochralski technique (JCPDS # 34-0097).

The strongest peak of the samples shifted to the lower diffraction angle, implying the lattice constant of 14BTO increased with the increasing sintering temperature. The calculated lattice constants for each case are shown in Fig. 2. In comparison with the lattice parameter of 10.175 Å from the single crystal $Bi_{12}TiO_{20}$ (JCPDS # 34-0097), the sintered 14BTO showed

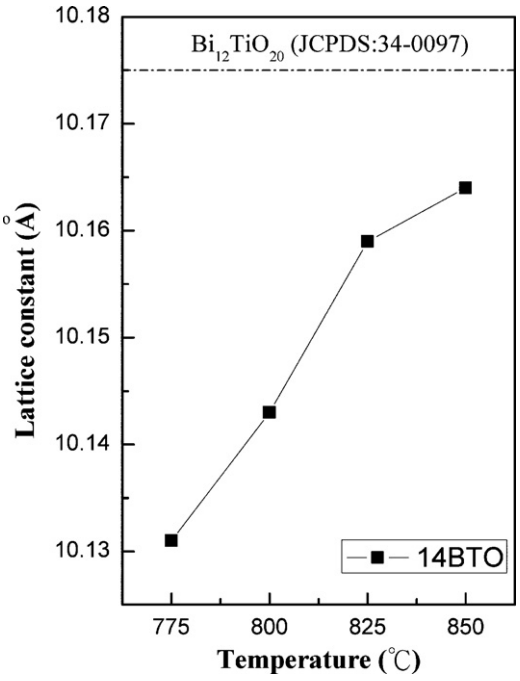

Fig. 2. Lattice constants of 14BTO samples sintered at various temperatures for 2 h.

smaller lattice parameters which decreases with sintering temperature from 10.164 Å at 850 °C to 10.115 Å at 775 °C. The variation in the lattice parameter can be an indication of the defect concentration in the crystal structure associated with change of temperature. TiO_2 is a material well known for the presence of its intrinsic defects at raised temperatures. It is possible that in the structure of $Bi_{12}TiO_{20}$ there are also an increased number of structural defects present at higher temperatures. The higher concentrations of lattice defects locally distort the lattice structure which leads to the average expansion of the lattice parameter as temperature increases. As such, explaining the variation of peak position for the four separately sintered samples.

3.2. Sintered densities

The densities of the samples were separately measured according to Archimedes method. The relative densities of the samples sintered from 775 °C to 850 °C are 50.02%, 52.66%, 66.50%, and 96.82%, respectively Comparing to die-pressing samples, the highest sintered density is 93.03% under 850 °C/2 h heat treatment, which is lower than the case by pressure filtration. Tekeli et al. previously reported on the investigation of die-pressed and pressure filtration sintered densities for mixed powders.[24] It has been shown that pressure filtration resulted in relatively higher sintered densities with a more uniform packing behavior. For maximized density of sintered pellet, sufficient temperature using pressure-filtration technique is preferred.

Plane view and cross sectional SEM images of the sintered samples are shown in Fig. 3. The grain sizes increased on average of 1.8–6.5 μm as sintering temperature increased from 775 °C to 850 °C. It is also evident that the porosity of 850 °C sintered sample corresponded to a high sintered density obtained by Archimedes method. The porosity derived from Archimedes method was 7.99% at a bulk density of 8.346 g cm^{-3}, while the porosity from the 2-D SEM micrograph was calculated to be 8.90%.

3.3. Electrical properties

Fig. 4 shows the Arrhenius plot of the conductivity of 14BTO sample determined by two-probe DC method. Bulk 8YSZ and Bi_2O_3 and single crystal $Bi_{12}TiO_{20}$ samples are also used for the comparison.[4,25,26] The conductivity of 14BTO sample was subpar to the common SOFC electrolyte material, i.e., 8YSZ which is capable of a few orders higher, but is higher than the pure α-monoclinic Bi_2O_3 below 730 °C. Above 730 °C, one-step conductivity feature of 14BTO sample represented a stable phase without any phase transition compared to pure Bi_2O_3. The crystalline structure of the $Bi_{12}TiO_{20}$ is sillenite, having tetrahedrally coordinated Ti^{4+} cations occupying the bcc sites while the Bi^{3+} taking the hepta-coordinated positions. The atom positions are relatively fixed compared to that of ionic conducting Bi_2O_3. Oxygen anions are considered to exhibit little mobility. In a study of similarly structured Bi_2O_3 based sillenites, those that represent perfect lattices have shown to result in the lowest conductivity values.[27] Apparently, this phenomenon was also true for $Bi_{12}TiO_{20}$ sillenites.

Several suggested the presence of intrinsic defects that may involve misplaced cations at higher temperatures.[28–30] The intrinsic defect may involve titanium-vacancy complex or bismuth cations misplacing the titanium cations at the bcc sites. The misplaced bismuth cations induce charge imbalance suggesting electron holes paired with bismuth cations at titanium cation sites. The defect-hole pair would result in a p-type electronic conduction. In the experimental analysis by Lanfredi et al.,[25,26] activation energy (Ea) of 0.99 eV which closely resembled that of semiconducting characteristics, is lower than that of 850 °C-sintered 14BTO sample in this study (Ea: 1.09 eV). However, the conductivity of single crystal $Bi_{12}TiO_{20}$ obtained by Lanfredi et al.,[25,26] revealing the higher values range from 5×10^{-6} and 9×10^{-4} S cm^{-1} in the temperature range of 400–700 °C as compared to our prepared samples. In our previous study, the grain boundaries of electrolytes possess a blocking effect of ionic conduction throughout the layers.[31] Thus, the lower conductivity can result as a greater disorder introduced to the sillenite structure due to introduction of grain boundaries. Disorder in the grain interior is also possible. In disordered 14BTO, where bismuth cations take up the bcc positions such as that of ionically conducting γ-Bi_2O_3,[32] there could be a mixed conduction due to oxygen vacancies. Either way, the conductivities were improved over the pure α-monoclinic Bi_2O_3 at the intermediate temperature range.

3.4. Long-term stability of $Bi_{12}TiO_{20}$

In addition to the thermal stability test, many studies that assess Bi_2O_3 based electrolytes seek long term stability. Jiang et al.[2] conducted experiments demonstrating conductivity decay

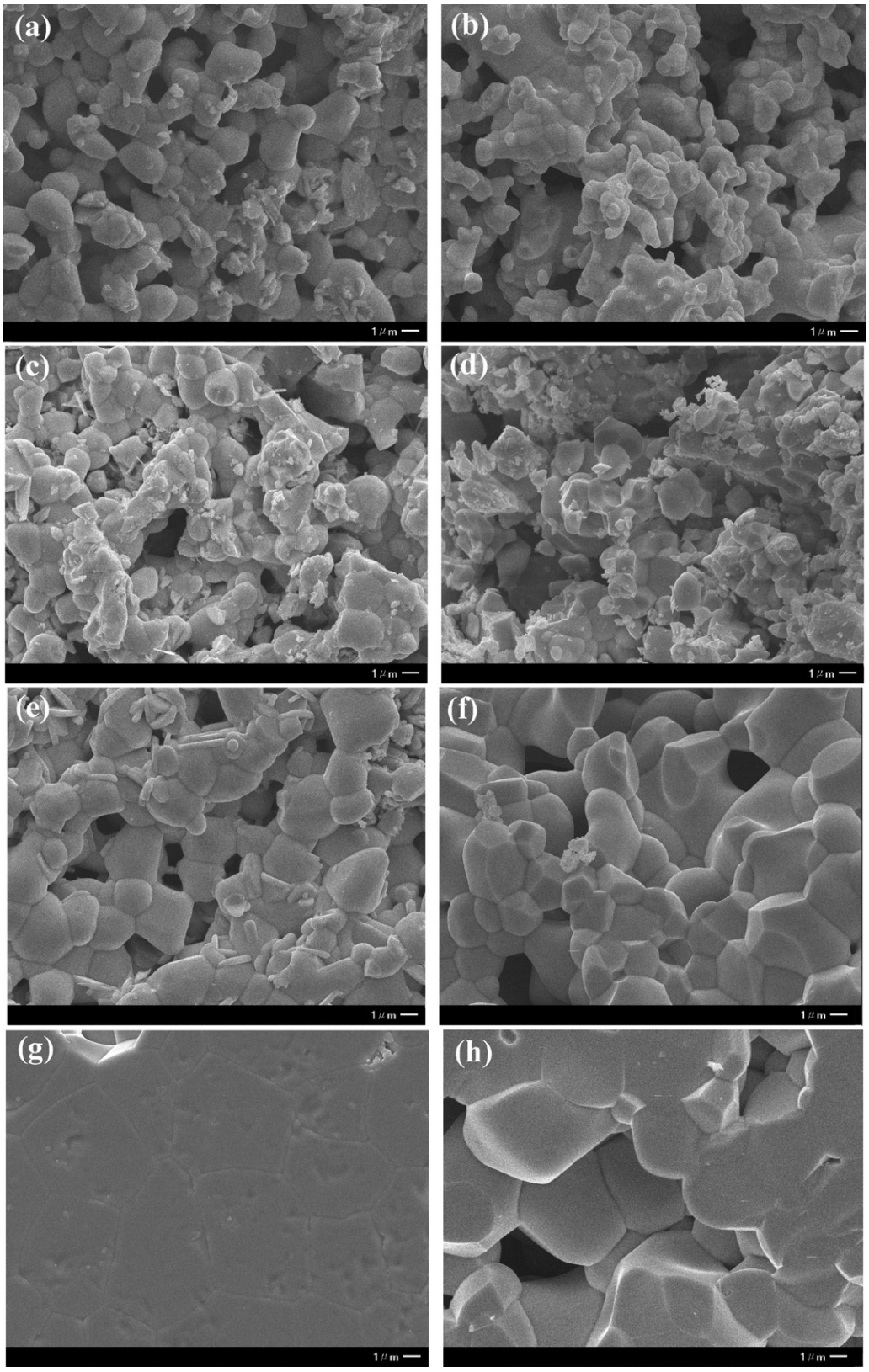

Fig. 3. SEM surface morphology of 14BTO samples sintered for 2 h at (a) 775 °C, (c) 800 °C, (e) 825 °C, (g) 850 °C, and cross-sectional microstructures sintered for 2 h at (b) 775 °C, (d) 800 °C, (f) 825 °C, and (h) 850 °C.

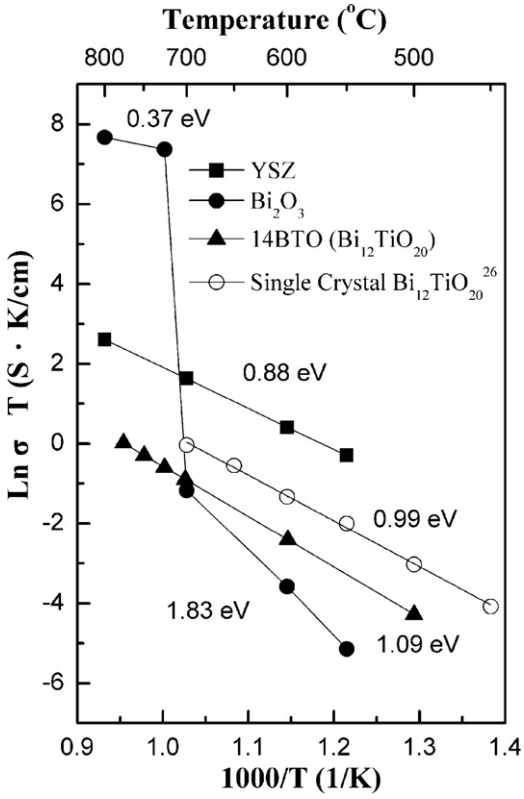

Fig. 4. Arrhenius plot of the conductivity as a function of temperatures for 850 °C-sintered 14BTO ($Bi_{12}TiO_{20}$) samples, bulk Bi_2O_3, YSZ and single crystal $Bi_{12}TiO_{20}$ samples.

over extended heating periods in the trivalent doped structures. In this study, 14BTO was held at 600 °C and two-probe DC conductivity was in situ measured up to 24 h. The variation of total conductivity with time is shown in Fig. 5. The conductivity experienced a drastic drop within the initial 6 h. Prolonged heating past 6 h became stabilized at about 0.7×10^{-4} S/cm.

Jiang et al.[2] thoroughly demonstrated a series of characteristic drastic initial downfall of the conductivity curves of M^{3+} doped Bi_2O_3 at raised temperatures as a reinvestigation of the work by Fung et al.[33–35] The M^{3+}s showed sign of greater conductivity degradation with decreasing dopant cation radii which was later proposed as the effect of the extent of cation polarizability.[10] The drastic initial down fall of the conductivity in the first 6 h was also characteristic with those structures reported in the literature.[8,2] This phenomenon was described by Fung et al. as structural ordering as a result of the face centered cubic (fcc)-rhombohedral transformation specifically conducted in their study of RE_2O_3–Bi_2O_3 (RE = Yb, Er, Y, or Dy) systems, which the rhombohedral phase in the RE_2O_3–Bi_2O_3 system resulted in a lower conductivity.[33–35] In the work conducted by Jiang et al.,[2] there were no apparent structural changes over the course of conductivity decay. Yet, the behavior may well reveal some kind of ordering or relaxation which can be reversed at the order–disorder transition temperature.[2] Starting with highly disordered fcc based bismuth oxides, the transition behavior may be best represented in cation ordering and anion or vacancy ordering. Cation ordering was proposed based on elastic diffuse neutron scattering that the Yb^{3+} cations may have restricted placements on the cube corners to lower the symmetry of the bismuth fcc lattice.[9] In addition, the polarizability of oxygen was found to have no effect on diffusion from classical mechanic simulations.[10] This means that ordering of the less polar dopant cations could result in the immobility of oxygen anions more so than the ordering of oxygen anions itself. In long term annealing, however, the ordering of oxygen vacancies will occur.[11,12]

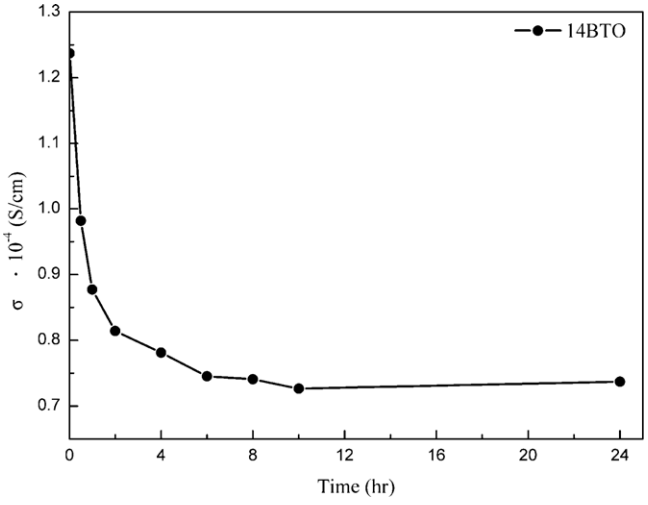

Fig. 5. Variation of total conductivity of 14BTO samples measured at 600 °C as a function of time.

For 14BTO sillenites, the conductivity decay can be associated with: (1) relaxation and reduction of the defect and disorder introduced at the grain boundaries, or (2) possibly interfacial reaction with the electrode materials. In order to verified the possible reasons of conductivity degradation, batch-type conductivity measurement from 400 °C to 700 °C as long as 1344 h were conducted as shown in Fig. 6. The results show no significant change neither in conductivity nor in activation energy, representing no phase separation or defect ordering was occurred during long-term treatment at 600 °C.

The furthermore examinations of crystalline structure by XRD with different treatment period at 600 °C were carried out as shown in Fig. 7. Even underwent 1344 h treatment at 600 °C, sample performed the same $Bi_{12}TiO_{20}$ sillenite phase. Comparing to batch-type conductivity measurement results as shown in Fig. 6, it is believed that the conductivity degradation from in situ experiment is due to interface interaction between sample and electrode. Therefore, the conductivity experienced a drastic fall within the initial 6 h. Once the interface formed a stable secondary phase, it became stabilized at about 0.7×10^{-4} S/cm as shown in Fig. 5.

3.5. Stability of $Bi_{12}TiO_{20}$ under CH_4 atmosphere

For practical application of SOFC electrolyte, the material should be stable in reduction atmosphere conduction. The reduction–oxidation tests of 14BTO at 700, 750 and 850 °C under 20% CH_4 atmosphere were carried out as shown in Fig. 8. Weight loss monitor for each case reveal an obvious loss of 1.5%, 3.5% and 5.6% for 700, 750 and 800 °C cases, respec-

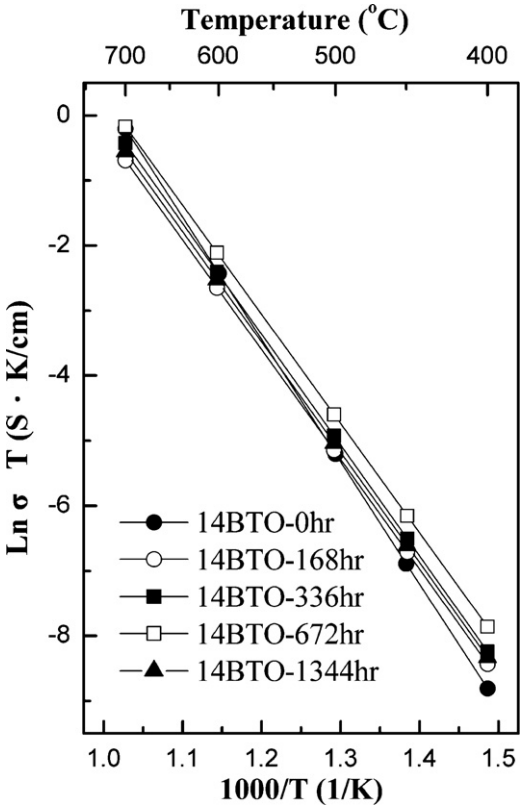

Fig. 6. Arrhenius plot of sintered 14BTO samples aging at 600 °C with different aging time.

tively. It means 14BTO would be reduced under this atmosphere condition. If pure air was purged into the chamber again, the weight of 14BTO would recover to its original condition at 700 °C (Fig. 8(a)). However, the non-reversible phenomenon were occurred at the conditions of 750 °C and 800 °C (Fig. 8 (b) and (c)), which are due to the reduction form of metallic bismuth species observed by XRD (not shown herein). Thus, it

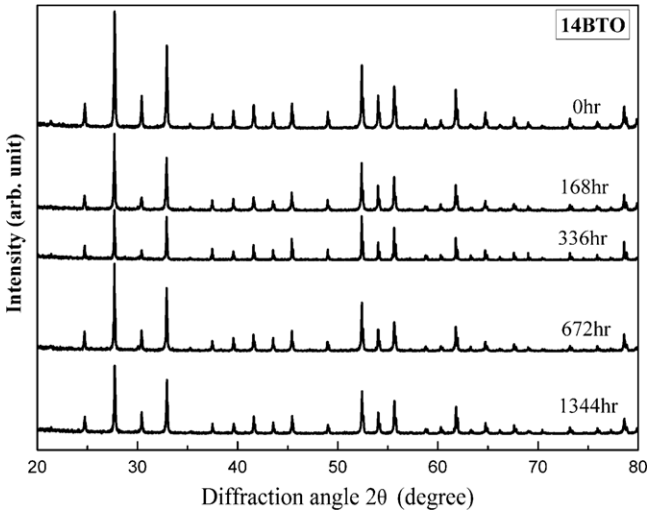

Fig. 7. XRD spectra of 14BTO samples aging at 600 °C with different aging time.

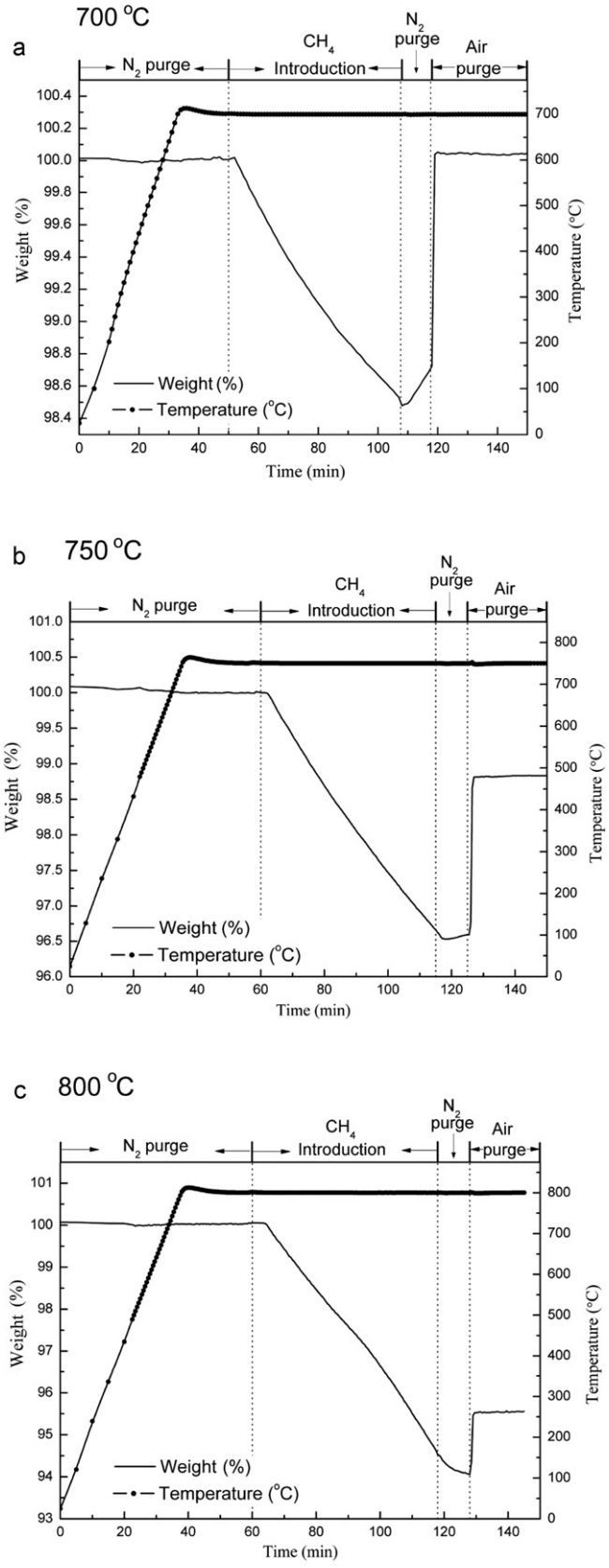

Fig. 8. Reduction–oxidation behaviors of 14BTO samples under various reaction temperatures; (a) 700 °C, (b) 750 °C, and (c) 800 °C.

could be concluded that the practical application of 14BTO as electrolytes should be below 700 °C under CH_4 atmosphere.

4. Conclusions

14BTO ($Bi_{12}TiO_{20}$) with a sillenite single phase was prepared through suitable colloid processing-pressure filtration methods and subsequent sintered at 775–850 °C for 2 h. The high relative sintered density of 96.82% was obtained at the sintering temperature of 850 °C. Conductivity measurement showed one step feature with the activation energy of 1.09 eV, representing 14BTO as a stable material at the range of operation temperatures of 500–775 °C without possible phase transition. The degradation on in situ conductivity measurement could be recognized as the higher interfacial resistance by the interaction between 14BTO and Pt electrode. Thus, both in situ and batch-type long-term conductivity measurements at 600 °C could illustrate the behavior of a good thermal stability of 14BTO samples without any sign of phase separation. Additionally, reduction–oxidation tests of 14BTO by TGA revealed possible upper application temperature is below 700 °C under CH_4 atmosphere.

Acknowledgement

The authors would like to thank the National Science Council of the Republic of China for financially supporting this research under contract no. NSC 99-2221-E-011-044.

References

1. Shuk P, Wiemhofer H-D, Guth U, Gopel W, Greenblatt M. Oxide ion conducting solid electrolytes based on Bi_2O_3. *Solid State Ionics* 1996;**89**:179–96.
2. Jiang N, Waschman ED. Structural stability and conductivity of phase-stabilized cubic bismuth oxides. *J Am Ceram Soc* 1999;**82**:3057–64.
3. Sammes NM, Tompsett GA, Nafe H, Aldinger F. Bismuth based oxide electrolytes-structure and ionic conductivity. *J Eur Ceram Soc* 1999;**19**:1801–26.
4. Laurent K, Wang GY, Tusseau-Nenez S, Leprince-Wang Y. Structure and conductivity studies of electrodeposited δ-Bi_2O_3. *Solid State Ionics* 2008;**178**:1735–9.
5. Iwahara H, Esaka T, Sato T, Takahashi T. Formation of high oxide ion conductive phases in the sintered oxides of the system Bi_2O_3–Ln_2O_3 (Ln = La–Yb). *J Solid State Chem* 1981;**39**:173–80.
6. Verkerk MJ, Van de Velde GMH, Burggraaf AJ. Structure and ionic conductivity of Bi_2O_3 substituted with lanthanide oxides. *J Phys Chem Solids* 1982;**43**:1129–36.
7. Dordor PJ, Tanaka J, Watanabe A. Electrical characterization of phase transition in yttrium doped bismuth oxide, $Bi_{1.55}Y_{0.45}O_3$. *Solid State Ionics* 1987;**25**:177–81.
8. Wachsman ED, Boyapati S, Jiang N. Effect of dopant polarizability on oxygen sublattice order in phase-stabilized cubic bismuth oxides. *Ionics* 2001;**7**:1–6.
9. Battle PD, Catlow CRA, Moroney LM. Structural and dynamical studies of δ-Bi_2O_3 oxide-ion conductors. II. A structural comparison of $(Bi_2O_3)_{1-x}(M_2O_3)_x$ for M = Y, Er, and Yb. *J Solid State Chem* 1987;**67**:42–50.
10. Aidhy DS, Sinnott SB, Wachsman ED, Phillpot SR. Effect of ionic polarizability on oxygen diffusion in δ-Bi_2O_3 from atomistic simulation. *Ionics* 2010;**16**:297–303.
11. Wachsman ED, Boyapati S, Kaufman M. Modeling of ordered structures of phase-stabilized cubic bismuth oxides. *J Am Ceram Soc* 2000;**83**:1964–8.
12. Boyapati S, Wachsman ED, Jiang N. Effect of oxygen sublattice ordering on interstitial transport mechanism and conductivity activation energies in phase-stabilized cubic bismuth oxides. *Solid State Ionics* 2001;**140**:149–60.
13. Jurado JR, Moure C, Duran P, Valverde N. Preparation and electrical properties of oxygen ion conductors in the Bi_2O_3-Y_2O_3 (Er_2O_3) systems. *Solid State Ionics* 1988;**518**:28–30.
14. Esaka T, Mangahara T, Iwahara H. Oxide ion conduction in the sintered oxides of the system Bi_2O_3–MO_2 (M = Ti, Sn, Zr, Te). *Solid State Ionics* 1989;**36**:129–32.
15. Takahashi T, Iwahara H, Esaka T. High oxide ion conduction in sintered oxide of the system Bi_2O_3–M_2O_5. *J Electrochem Soc* 1977;**124**:1563–9.
16. Bruton TM. Study of the liquidus in the system Bi_2O_3–TiO_2. *J Solid State Chem* 1974;**9**:173–5.
17. Xie L, Ma J, Tian H, Zhou J, Zhao Z, Wu P, et al. Isopropanol-assisted hydrothermal synthesis of bismuth titanate nanophotocatalysts. *Mater Lett* 2006;**60**:284–6.
18. Xu S, Shangguan W, Yuan J, Shi J, Chen M. Photocatalytic properties of bismuth titanate $Bi_{12}TiO_{20}$ prepared by co-precipitation processing. *Mater Sci Eng B* 2007;**137**:108–11.
19. Yao WF, Wang H, Xu XH, Zhou JT, Yang XN, Zhang Y, et al. Sillenites materials as novel photocatalysts for methyl orange decomposition. *Chem Phys Lett* 2003;**377**:501–6.
20. Yao WF, Wang H, Xu XH, Cheng XF, Huang J, Shang SX, et al. Photocatalytic property of bismuth titanate $Bi_{12}TiO_{20}$ crystals. *Appl Catal A: Gen* 2003;**243**:185–90.
21. Zhou J, Zou Z, Ray AK, Zhao XS. Preparation and characterization of polycrystalline bismuth titanate $Bi_{12}TiO_{20}$ and its photocatalytic properties under visible light irradiation. *Ind Eng Chem Res* 2007;**46**:745–9.
22. Weng CH, Wei WCJ. Synthesis and properties of homogeneous Nb-doped bismuth oxide. *J Am Ceram Soc* 2010;**93**:3124–9.
23. Lin SE, Kuo YL, Chou CH, Wei WCJ. Characterization of electrolyte films deposited by using RF magnetron sputtering a 20 mol% gadolinia-doped ceria target. *Thin Solid Films* 2010;**518**:7229–32.
24. Tekeli S, Demir U. Colloidal processing, sintering and static grain growth behavior of alumina-doped cubic zirconia. *Ceram Int* 2005;**31**:973–80.
25. Lanfredi S, Carvalho JF, Hernandes AC. Electric and dielectric properties of $Bi_{12}TiO_{20}$ single crystals. *J Appl Phys* 2000;**88**:283–7.
26. Lanfredi S, Nobre MAL. Conductivity mechanism analysis at high temperature in bismuth titanate: a single crystal with sillenite-type structure. *Appl Phys Lett* 2005;**86**:1–3.
27. Kilner JA, Drennan J, Dennis P, Steele BCH. A study of anion transport in bismuth based oxide systems by electrical conductivity and secondary ion mass spectroscopy (SIMS). *Solid State Ionics* 1981;**5**:527–30.
28. Efendiev SHM, Bagiev VE, Zeinally ACH, Balashov VA, Lomonov VA, Majer AA. Optical properties of $Bi_{12}TiO_{20}$ single crystals. *Phys Status Solidi A* 1981;**63**:K19–22.
29. Carvalho JF, Franco RWA, Magon CJ, Nunes LAO, Pellegrini F, Hernandes AC. Vanadium characterization in BTO: V sillenite crystals. *Mater Res* 1999;**2**:89–91.
30. Oberschmid R. Absorption centers of $Bi_{12}GeO_{20}$ and $Bi_{12}SiO_{20}$ crystals. *Phys Status Solidi A* 1985;**89**:263–70.
31. Kuo YL, Lee C, Chen YS, Liang H. Gadolinia-doped ceria films deposited by RF reactive magnetron sputtering. *Solid State Ionics* 2009;**180**:1421–8.
32. Harwig HA, Gerards AG. Electrical properties of the α, β, γ, and δ phases of bismuth sesquioxide. *J Solid State Chem* 1978;**26**:265–74.
33. Fung KZ, Virkar AV. Phase stability, phase transformation kinetics, and conductivity of Y_2O_3–Bi_2O_3 solid electrolytes containing aliovalent dopants. *J Am Ceram Soc* 1991;**74**:1970–80.
34. Fung KZ, Baek HD, Virkar AV. Thermodynamic and kinetic considerations for Bi_2O_3-based electrolytes. *Solid State Ionics* 1992;**52**:199–211.
35. Fung KZ, Chen J, Virkar AV. Effect of aliovalent dopants on the kinetics of phase transformation and ordering in RE_2O_3–Bi_2O_3 (RE = Yb, Er, Y, or Dy) solid solutions. *J Am Ceram Soc* 1993;**76**:2403–18.